Journal of Engineering Mathematics 20: 307–322 (1986)

Hydromechanics of low-Reynolds-number flow. Part 6. Rotation of oblate bodies

L.H. HUANG and A.T. CHWANG

Iowa Institute of Hydraulic Research, The University of Iowa, Iowa City, Iowa 52242, USA

(Received May 27, 1986)

Summary

Uniform ring distributions of fundamental singularities for Stokes flows, Stokeslets and rotlets, are applied to obtain exact solutions for rotating oblate bodies in an unbounded viscous fluid. The technique used in the present investigation is the inverse-problem approach. Instead of determining the types of singularities and their spatial distributions for a given body geometry, the body shape is determined for a given distribution of singularities. The rotating axis of a body is perpendicular to the plane containing the ring and it passes through the center of the circular ring. The direction of rotlets is parallel to the rotating axis, while the Stokeslets are tangent to the ring and lie in its plane. By changing the radius of the ring and/or changing the strengths of Stokeslets and rotlets, we obtain a family of rotating oblate bodies including simply-connected and doubly-connected bodies. Two special cases involving a slightly deformed sphere and a spinning slender torus are also discussed.

1. Introduction

We are concerned in this paper with the rotation of an axisymmetric oblate body in an incompressible, inertialess fluid. The governing equations for the resultant flow surrounding a rotating oblate body, if the fluid inertia is neglected, are the Stokes equations. As mentioned in the second part (Chwang and Wu [4]) of this series of papers on low-Reynolds-number flows, determination of the solutions for the Stokes flow is still recognized to be difficult in general for arbitrary body shapes. As a consequence, not many exact solutions are known.

Adopting an oblate spheroidal coordinate system and some rather sophisticated analysis of associated Legendre functions, Jeffery [6] obtained the solution for the velocity field and the torque resisting the rotation of an oblate spheroid. Kanwal [8] analyzed the flow surrounding a rotating torus by introducing a toroidal coordinate system. His solutions for the velocity field and the torque experienced by the torus were expressed in terms of infinite series involving Legendre functions. Based on the similar boundary-value approach, Brenner [1] solved the Stokes-flow problem for a slightly deformed sphere. Dorrepaal et al. [5] obtained an integral solution involving modified Bessel functions for the rotation of a closed torus, formed from the rotation of two equal touching circles about their common tangent.

An alternative yet powerful method of solving the Stokes equations is the singularity method. Chwang and Wu [4] and Chwang [2] have successfully applied the singularity

method to obtain many exact solutions for Stokes flows of various free-stream conditions past bodies of various geometric shapes. In this method, fundamental singularities such as Stokeslets and rotlets are distributed in the interior of a solid body in order to represent a given motion of the body. With a line distribution of rotlets, Chwang and Wu [3] constructed a number of exact solutions for the purely rotational flow generated by the rotation of axisymmetric prolate bodies of various shapes about their longitudinal axes. Johnson and Wu [7] investigated the Stokes flow past a slender torus of circular cross-section. With a line distribution of Stokeslets and rotlets on the body centre-line, they obtained an approximate solution for a rotating slender torus.

In the present paper, we construct exact solutions for rotating oblate bodies in an unbounded inertialess fluid with uniform ring distributions of Stokeslets and rotlets. The technique used in the present investigation is the inverse-problem approach. Instead of determining the types of singularities and their spatial distributions for a given body geometry, the body shape is determined for a given distribution of singularities. By changing the radius of the distribution ring and/or changing the strengths of Stokeslets and rotlets, we obtain a family of rotating oblate bodies including simply-connected and doubly-connected bodies. The limiting cases of a slightly deformed sphere and a slender torus are also discussed.

2. Ring distribution of singularities

With the inertia force being neglected, the velocity $\boldsymbol{u}$ and pressure p of an incompressible viscous fluid surrounding a rotating oblate body satisfy the Stokes equations

$$\nabla \cdot \boldsymbol{u} = 0, \quad \nabla p = \mu \nabla^2 \boldsymbol{u}, \tag{1}$$

where μ is the constant viscosity coefficient. On the body surface S_b, the no-slip boundary condition requires

$$\boldsymbol{u} = \boldsymbol{\omega} \times \boldsymbol{x} \quad \text{for } \boldsymbol{x} \text{ on } S_b, \tag{2a}$$

and far away from the body

$$\boldsymbol{u} = 0 \quad \text{as } \boldsymbol{x} \to \infty, \tag{2b}$$

where $\boldsymbol{\omega}$ is the angular velocity and $\boldsymbol{x}$ is the position vector in a three-dimensional Euclidean space. If we take the rotating axis of an oblate body to be the z axis, then

$$\boldsymbol{\omega} = \omega \boldsymbol{e}_z, \tag{2c}$$

where $\boldsymbol{e}_z$ is the unit vector along the z direction.

With a uniform ring distribution of Stokeslets and rotlets on a circle in the x, y plane, centered at the origin with radius c (Figure 1), the velocity vector $\boldsymbol{u}$ is given by

$$\boldsymbol{u}(\boldsymbol{x}) = \int_c [\boldsymbol{u}_s(\boldsymbol{x} - \boldsymbol{\xi};\ \boldsymbol{\alpha}) + \boldsymbol{u}_R(\boldsymbol{x} - \boldsymbol{\xi};\ \boldsymbol{\beta})]\, c\, \mathrm{d}\phi, \tag{3}$$

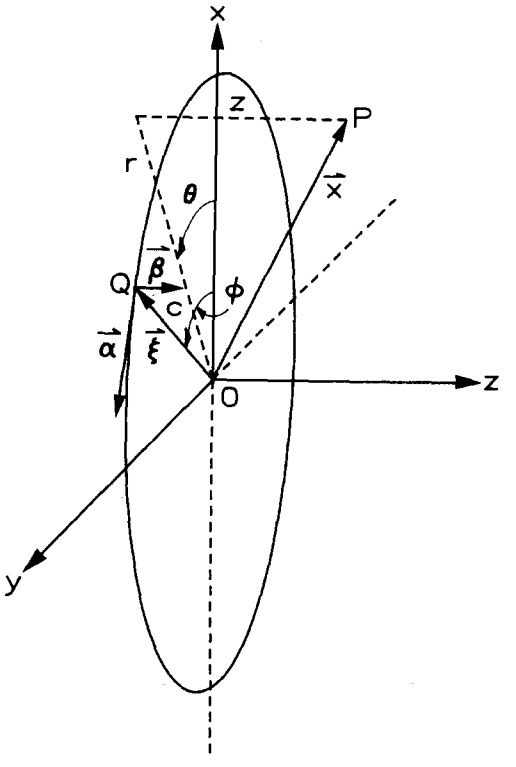

Figure 1. Orientation of the coordinate system.

where the position vector $\boldsymbol{x}$ of a field point P is

$$\boldsymbol{x} = r\cos\theta\boldsymbol{e}_x + r\sin\theta\boldsymbol{e}_y + z\boldsymbol{e}_z, \tag{4a}$$

the position vector $\boldsymbol{\xi}$ of a point Q on the ring is

$$\boldsymbol{\xi} = c\cos\phi\boldsymbol{e}_x + c\sin\phi\boldsymbol{e}_y, \tag{4b}$$

and the velocity fields of a Stokeslet and a rotlet are given by

$$\boldsymbol{u}_s(\boldsymbol{x};\ \boldsymbol{\alpha}) = \frac{\boldsymbol{\alpha}}{R} + \frac{(\boldsymbol{\alpha}\cdot\boldsymbol{x})\boldsymbol{x}}{R^3} \tag{4c}$$

and

$$\boldsymbol{u}_R(\boldsymbol{x};\ \boldsymbol{\beta}) = \frac{\boldsymbol{\beta}\times\boldsymbol{x}}{R^3}, \tag{4d}$$

respectively, with

$$R = |\boldsymbol{x}|. \tag{4e}$$

The vectorial strengths of the Stokeslets and rotlets are selected such that the direction of rotlets is parallel to the z axis,

$$\boldsymbol{\beta} = \beta \boldsymbol{e}_z, \tag{4f}$$

while the Stokeslets are tangent to the ring and lie in the x, y plane,

$$\boldsymbol{\alpha} = \alpha \boldsymbol{e}_\phi, \tag{4g}$$

where $\boldsymbol{e}_\phi$ is a unit vector in the angular direction in the x, y plane (Figure 1). In terms of a cylindrical polar coordinate system (r, θ, z),

$$\boldsymbol{e}_\phi = \cos(\phi - \theta)\boldsymbol{e}_\theta - \sin(\phi - \theta)\boldsymbol{e}_r, \tag{4h}$$

where $\boldsymbol{e}_\theta$ and $\boldsymbol{e}_r$ are unit vectors along the θ and r directions respectively.

Integrating equation (3) from $\phi = \theta - \pi$ to $\phi = \theta + \pi$ and using the relations (4a) to (4h), we have

$$\boldsymbol{u}(\boldsymbol{x}) = u_\theta \boldsymbol{e}_\theta, \tag{5a}$$

$$u_\theta = \frac{2\beta c}{rR_1}\left[\frac{r^2 - z^2 - c^2}{z^2 + (r-c)^2}E(k) + K(k)\right] + \frac{4\alpha R_1}{r}\left[\frac{z^2 + r^2 + c^2}{R_1^2}K(k) - E(k)\right], \tag{5b}$$

where

$$R_1 = \left[z^2 + (r+c)^2\right]^{1/2}, \tag{5c}$$

$$k^2 = \frac{4rc}{R_1^2}, \tag{5d}$$

$K(k)$ and $E(k)$ are the complete elliptic integrals of the first and second kinds, respectively,

$$K(k) = \int_0^{\pi/2} (1 - k^2 \sin^2\phi)^{-1/2}\, \mathrm{d}\phi, \tag{6a}$$

$$E(k) = \int_0^{\pi/2} (1 - k^2 \sin^2\phi)^{1/2}\, \mathrm{d}\phi. \tag{6b}$$

3. Determination of body shape

In terms of the cylindrical polar coordinate system (r, θ, z), the surface of an axisymmetric oblate body is given by

$$r = r_0(z), \tag{7a}$$

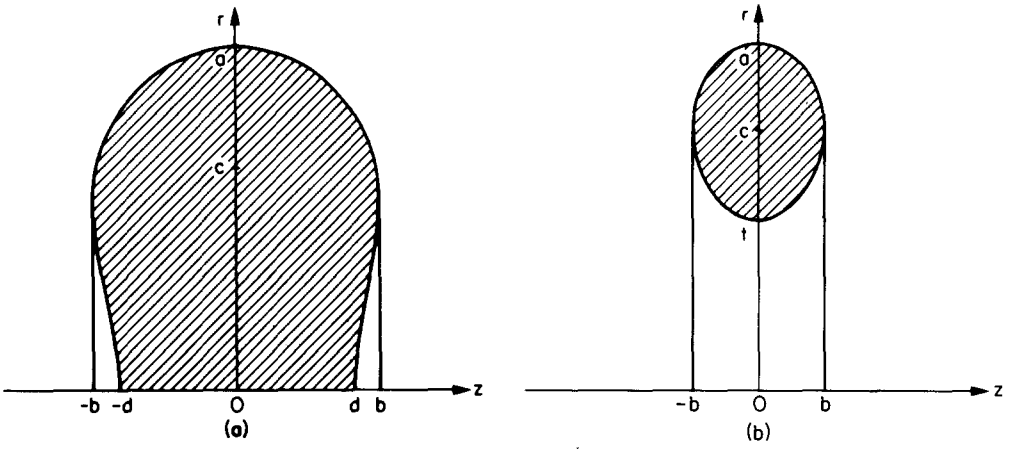

Figure 2. Sectional view of an axisymmetric oblate body: (a) a class-A body, (b) a class-B body.

and the maximum radius of the body is denoted by a, which occurs at the $z = 0$ plane (Figure 2)

$$r_0(0) = a \quad (a > c \geqslant 0). \tag{7b}$$

The no-slip boundary condition (2a) together with (2c) becomes

$$u_\theta = \omega r \quad \text{on } r = r_0(z). \tag{8}$$

By equations (5) and (8), we obtain an implicit equation for the body surface $r_0(z)$,

$$\frac{\omega a^3}{\beta c} = \frac{2a^3}{r^2 R_1}\left[\frac{r^2 - z^2 - c^2}{z^2 + (r-c)^2}E(k) + K(k)\right] + \frac{4a^2 R_1}{cer^2}\left[\frac{z^2 + r^2 + c^2}{R_1^2}K(k) - E(k)\right]$$

$$\text{on } r = r_0(z), \tag{9a}$$

where

$$e = \frac{\beta}{a\alpha}. \tag{9b}$$

For given values of c/a and e, equation (9) provides an implicit relation to determine the body surface r_0/a as a function of z/a with the left-hand side of (9a) determined by the condition (7b) as

$$\frac{\omega a^3}{\beta c} = \frac{2a}{a+c}\left[\frac{a+c}{a-c}E(k_0) + K(k_0)\right] + \frac{4(a+c)}{ce}\left[\frac{a^2 + c^2}{(a+c)^2}K(k_0) - E(k_0)\right], \tag{10a}$$

where

$$k_0^2 = \frac{4ac}{(a+c)^2}. \tag{10b}$$

Equations (9) and (10) can be solved numerically by the Newton-Raphson method to give the body shape $r_0(z)/a$ which depends on the values of the ring size c/a and the singularity-strength ratio e. Alternatively, we may obtain from (9) and (10) the body surface z/a as a function of r_0/a. The dimensionless ring size c/a varies from zero to one and the range for e is from zero to infinity. When e is equal to zero, we have a ring distribution of uniform Stokeslets. On the other hand, as e approaches infinity, we have a ring distribution of uniform rotlets only.

4. Classification of body shapes

We classify the shapes of axisymmetric oblate bodies into two categories:

(1) Class A – simply connected bodies (Figure 2a),

(2) Class B – doubly connected bodies (Figure 2b).

A class-A body resembles the shape of a red blood-cell, while a class-B body looks like a doughnut.

When the dimensionless ring size c/a is between zero and 0.4411 ($0 \leqslant c/a \leqslant 0.4411$), the numerical results obtained from equations (9) and (10) indicate that only class-A bodies exist for arbitrary values of e ($0 \leqslant e < \infty$). Figure 3 shows the body shapes at $c/a = 0.1$ and Figure 4 shows the body shapes at $c/a = 0.4411$. We note that as c/a tends to zero, equation (9a) reduces to

$$\frac{\omega a^3}{\beta c} = \frac{2\pi a^3}{(z^2 + r_0^2)^{3/2}}\left[1 + \frac{c}{ea} + O\left(\frac{c}{a}\right)^2\right], \tag{11a}$$

and (10a) reduces to

$$\frac{\omega a^3}{\beta c} = 2\pi\left[1 + \frac{c}{ea} + O\left(\frac{c}{a}\right)^2\right]. \tag{11b}$$

Therefore, by neglecting terms of the order of $(c/a)^2$, the equation for the body surface becomes

$$z^2 + r_0^2 = a^2 \quad \text{as } c/a \to 0, \tag{11c}$$

which is the same as that for a sphere of radius a.

For $0.4411 < c/a \leqslant 0.6637$, only class-A bodies exist, but the range of e is limited to $0 \leqslant e < e_1$, where $e_1 < \infty$. If e is greater than e_1, no solutions are possible for fixed values of c/a ($0.4411 < c/a \leqslant 0.6637$). Figure 5 shows examples of body shapes at $c/a = 0.5$.

The surface of a class-A body intersects the z axis at $-d$ and d (Figure 2a). Hence the

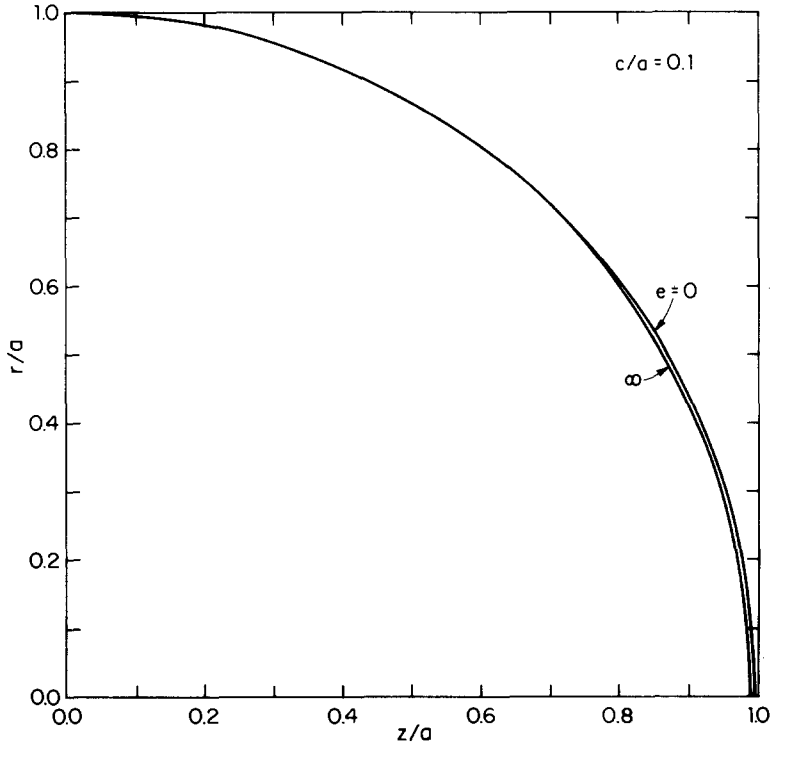

Figure 3. Body shapes for $c/a = 0.1$.

existence of d $(0 < d \leqslant a)$ is a necessary condition for the existence of a class-A body. Since r_0 $(\pm d) = 0$, equations (9) and (10) yield, in the limit as r tends to zero,

$$F_1(d/a;\ c/a,\ e) = \frac{\pi a^3}{(d^2+c^2)^{5/2}}\left[(d^2+c^2)\left(1+\frac{c}{ea}\right)-\tfrac{3}{2}c^2\right]$$
$$-\frac{a}{a+c}\left[\frac{a+c}{a-c}E(k_0)+K(k_0)\right]$$
$$-\frac{2(a+c)}{ce}\left[\frac{a^2+c^2}{(a+c)^2}K(k_0)-E(k_0)\right]=0, \tag{12}$$

where k_0 is given by (10b). Thus, d is the positive root of equation (12). At $c = 0$, the solution of (12) is $d = a$ regardless the values of e, which corresponds to a sphere of radius a. This result is consistent with (11c) with $r_0 = 0$.

For fixed values of e, the numerical result of (12) indicates that d/a decreases as c/a increases. This is also shown in Figures 3 and 4. For fixed values of c/a, d/a (which is the value of z/a at $r = 0$) decreases as e increases; it attains a minimum value as e approaches infinity. If d_m denotes the minimum value of d at which $\partial F_1/\partial d = 0$, we obtain from (12), as e tends to infinity,

$$d_m = (3/2)^{1/2}c. \tag{13a}$$

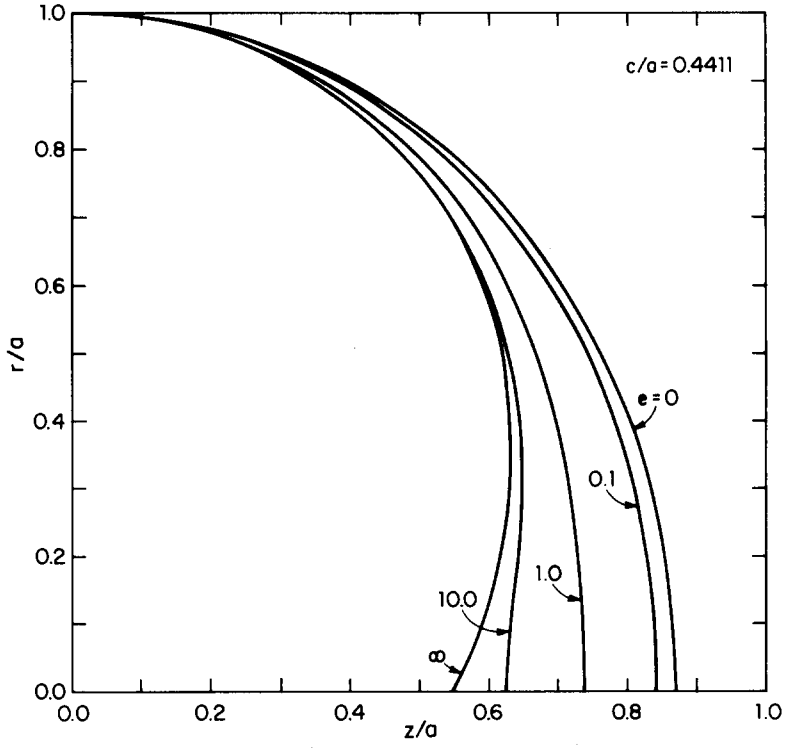

Figure 4. Body shapes for $c/a = 0.4411$.

Substituting (13a] into [12], we have

$$d_m/a = 0.5403 \quad \text{and } c/a = 0.4411 \text{ as } e \to \infty. \tag{13b}$$

Therefore, as e approaches infinity, the maximum value c/a may have is 0.4411. As c/a increases from zero to 0.4411, d/a decreases from 1 to 0.5403 (see Figure 4).

For c/a greater than 0.4411, although there is no solution for d_m from equation (12) as e tends to infinity, there is a possible solution if e is in the range between 0 and e_1 ($e_1 < \infty$). From (12), $\partial F_1/\partial d$ vanishes at $d = d_m$,

$$d_m = c\left[\left(\frac{3}{2} - \frac{c}{ea}\right)\Big/\left(1 + \frac{c}{ea}\right)\right]^{1/2}. \tag{14a}$$

Substituting (14a) into (12), we have an implicit equation for e_1 as a function of c/a,

$$F_1(d_m/a;\ c/a,\ e_1) = 0 \quad \text{for } \frac{3}{2} - \frac{c}{e_1 a} \geqslant 0. \tag{14b}$$

For example, for $c/a = 0.5$, e_1 is 1.6124 and the corresponding value of d_m/a is 0.4765 (see Figure 5). For a class-A body, the smallest possible value of d_m is zero which occurs at $c/a = 0.6637$, and the corresponding value of e_1 is 0.4425 (see Figure 6).

For c/a greater than 0.6637, both class-A and class-B bodies are possible. Examples of body shapes are shown in Figure 7 for $c/a = 0.7$. We note from Figure 7 that even for a class-B body, the singularity-strength ratio e cannot exceed a certain limiting value e_1

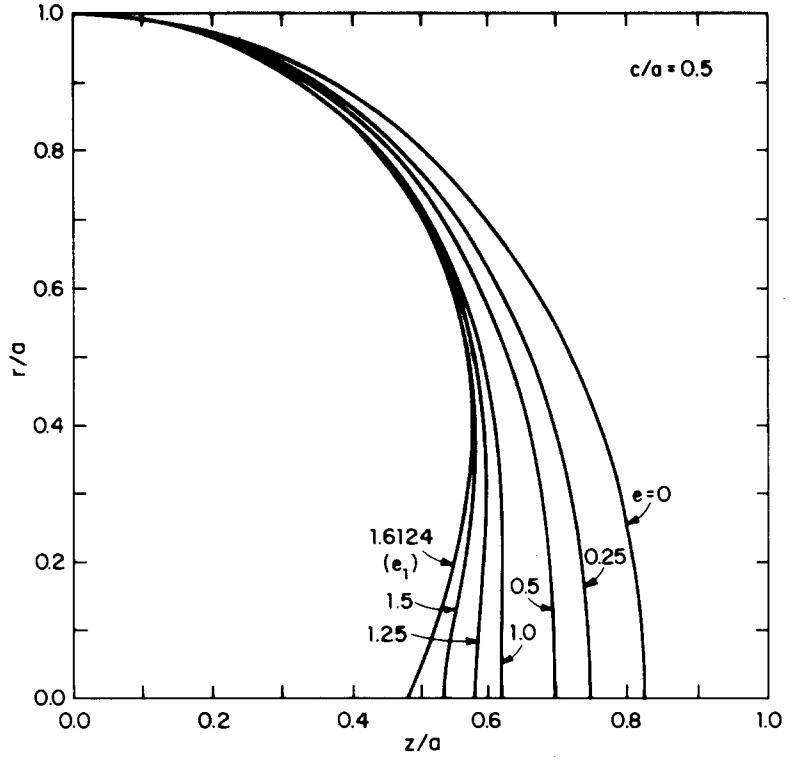

Figure 5. Body shapes for $c/a = 0.5$.

($e_1 = 0.3720$ at $c/a = 0.7$) which will be discussed in the next paragraph. For fixed values of c/a, d/a attains a maximum at $e = 0$, which represents a ring distribution of uniform Stokeslets only. As mentioned before, for any fixed value of e, d/a decreases as c/a increases for a class-A body (see Figure 3 to Figure 7). For $e = 0$ and $d = 0$, equation (12) gives

$$c/a = 0.8585 \quad \text{at } e = 0 \quad \text{and } d = 0. \tag{15}$$

Therefore, for $0.6637 < c/a < 0.8585$, both class-A and class-B bodies are possible, depending on the values of e. The class-A body and the class-B body are separated by a curve with $e = e_2$ which is determined from (12) at $d = 0$ (see Figure 8).

For $0.8585 \leqslant c/a < 1$, only class-B bodies are possible for $0 \leqslant e < e_1$. The surface of a class-B body intersects the r axis at $r_0 = t$ in addition to $r_0 = a$ (see Figure 2b). Therefore at $z = 0$, equations (9a) and (10a) give

$$F_2(t/a;\, c/a,\, e)$$

$$= \frac{a^3}{t^2(t+c)}\left[\frac{t+c}{t-c}E(k_1) + K(k_1)\right] + \frac{2a^2(t+c)}{cet^2}\left[\frac{t^2+c^2}{(t+c)^2}K(k_1) - E(k_1)\right]$$

$$- \frac{a}{a+c}\left[\frac{a+c}{a-c}E(k_0) + K(k_0)\right] - \frac{2(a+c)}{ce}\left[\frac{a^2+c^2}{(a+c)^2}K(k_0) - E(k_0)\right] = 0, \tag{16a}$$

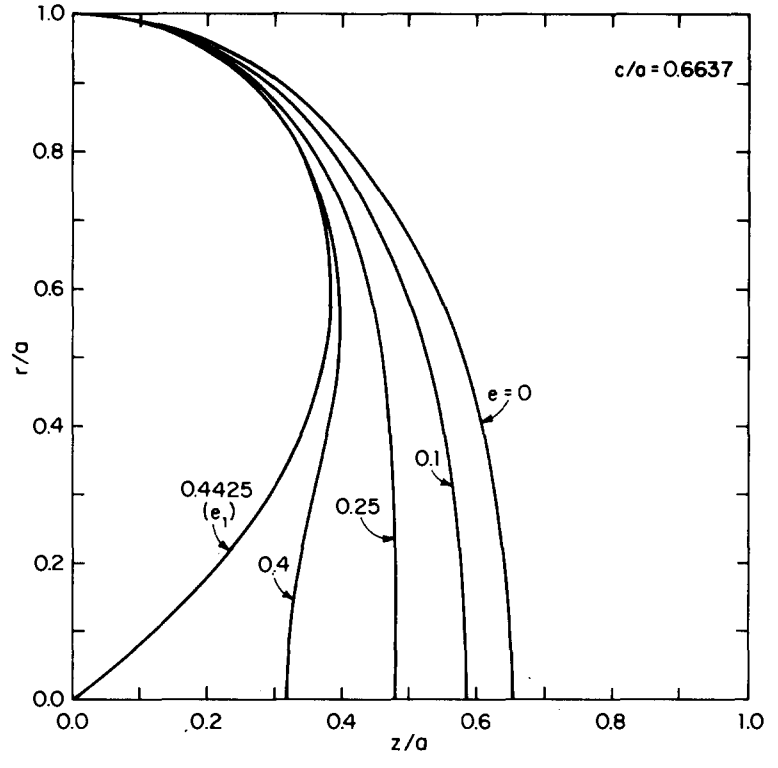

Figure 6. Body shapes for $c/a = 0.6637$.

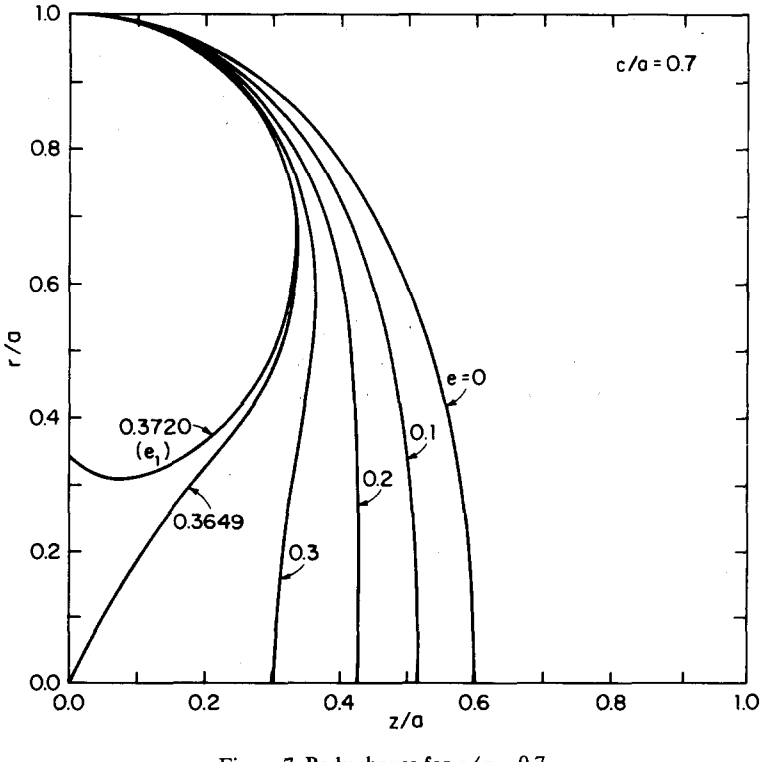

Figure 7. Body shapes for $c/a = 0.7$.

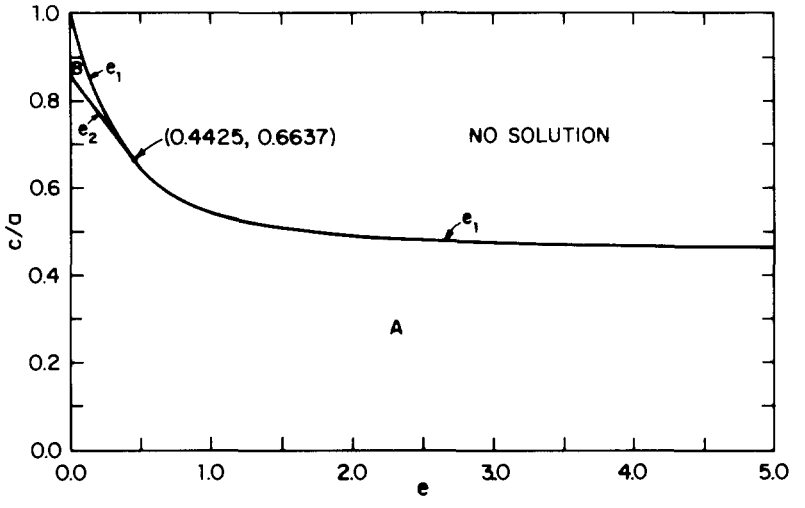

Figure 8. Classification of body shapes.

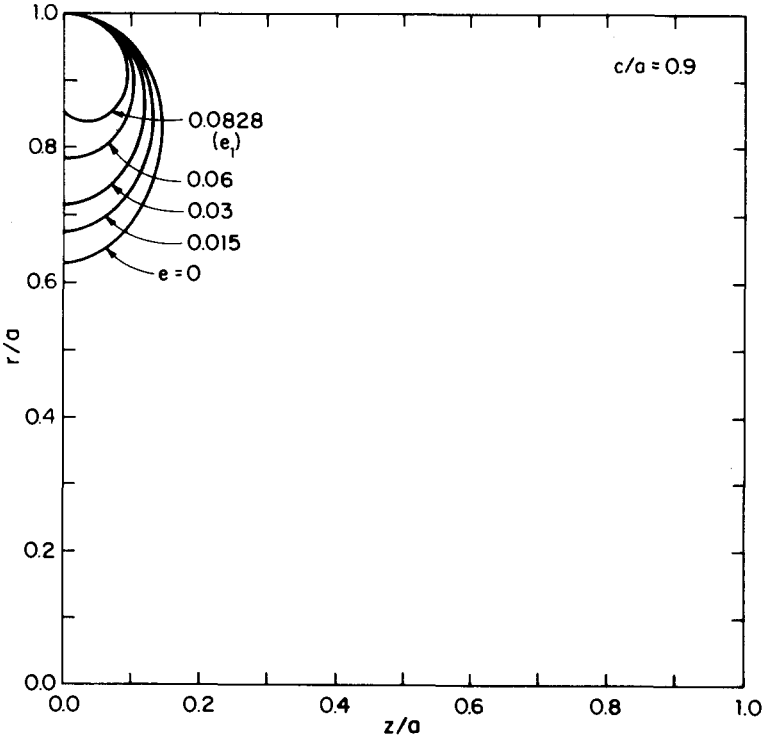

Figure 9. Body shapes for $c/a = 0.9$.

where

$$k_1^2 = \frac{4tc}{(t+c)^2} \tag{16b}$$

and k_0^2 is given by (10b). If t_m $(< a)$ denotes the maximum value of t at which $\partial F_2/\partial t = 0$, then the solution of the simultaneous equations

$$F_2(t_m/a;\ c/a,\ e_1) = 0 \quad \text{and} \quad \frac{\partial F_2}{\partial t}(t_m/a;\ c/a,\ e_1) = 0 \tag{17}$$

gives the limiting value of e_1 as a function of c/a. Numerical solutions of (17) are shown in Figure 8 for $0.6637 < c/a < 1$. Figure 9 shows examples of class-B bodies at $c/a = 0.9$, in which case the limiting value of e_1 is 0.0828.

5. The moment coefficient

The net force exerted by the fluid on a point Stokeslet with a vectorial strength $\boldsymbol{\alpha}$ is $-8\pi\mu\boldsymbol{\alpha}$ (see Chwang and Wu [4]). Therefore, for a ring distribution of uniform Stokeslets with a strength density $\alpha \boldsymbol{e}_\phi$ (equation (4g)), the net force on the body vanishes due to the symmetry of the ring and the antisymmetry of the strength density. Similarly, the pressure outside an axisymmetric oblate body rotating about the symmetry axis is constant throughout the fluid domain.

The net moment (or torque) on the oblate body due to a ring distribution of uniform Stokeslets does not vanish, it is in the negative z direction with a magnitude

$$M_s = 8\pi\mu\alpha(2\pi c)c = 16\pi^2\mu\alpha c^2. \tag{18a}$$

On the other hand, the net moment on the oblate body due to a ring distribution of uniform rotlets with density $\beta \boldsymbol{e}_z$ is also in the negative z direction with a magnitude (see Chwang and Wu [3])

$$M_R = 8\pi\mu\beta(2\pi c) = 16\pi^2\mu\beta c. \tag{18b}$$

Therefore, the total moment on the rotating oblate body is

$$\boldsymbol{M} = -M\boldsymbol{e}_z, \quad M = M_s + M_R. \tag{18c}$$

The moment coefficient C_m, normalized with respect to $8\pi\mu\omega a^2 b$, is

$$C_m = 2\pi\left(1 + \frac{c}{ea}\right)\beta c/(\omega a^2 b), \tag{19}$$

where b is the maximum half-thickness of an axisymmetric oblate body (see Figure 2) and $\omega a^3/\beta c$ is given by (10).

As e tends to zero, the body is generated by a ring distribution of uniform Stokeslets only. For this limiting case, (19) reduces to

$$\lim_{e\to 0} C_m = \frac{\pi c^2}{2b(a+c)}\left[\frac{a^2+c^2}{(a+c)^2}K(k_0) - E(k_0)\right]^{-1}, \tag{20}$$

where

$$k_0^2 = \frac{4ac}{(a+c)^2}. \tag{10b}$$

For $0 \leqslant c/a \leqslant 0.4411$, the singularity ratio e may vary from zero to infinity. As e approaches infinity, (19) becomes

$$\lim_{e\to\infty} C_m = \frac{\pi(a+c)}{b}\left[\frac{a+c}{a-c}E(k_0) + K(k_0)\right]^{-1}. \tag{21}$$

for c/a greater than 0.4411, the value of e is limited to the range of $0 \leqslant e < e_1$, where e_1 is obtained from (14b) for $0.4411 < c/a \leqslant 0.6637$ and from (17) for $0.6637 \leqslant c/a < 1$.

The moment coefficient C_m as computed from (20) and (21) is plotted in Figure 10 versus the spacing ratio c/a. For c/a greater than 0.4411, the moment coefficient curve C_m for $e \to \infty$ is connected to the curve at $e = e_1$. We may interpret that the entire lower curve in Figure 10 is evaluated at $e = e_1$, with e_1 equal to infinity for $0 \leqslant c/a \leqslant 0.4411$. For any other values of e between zero and e_1, the value of C_m lies in the region bounded by the two limiting curves at $e = 0$ and $e = e_1$ in Figure 10. We note from Figure 10 that $C_m = 1$ at $c/a = 0$, which represents the moment coefficient for a sphere. For fixed e, C_m increases monotonically as c/a increases, and it increases as e increases for fixed values of c/a.

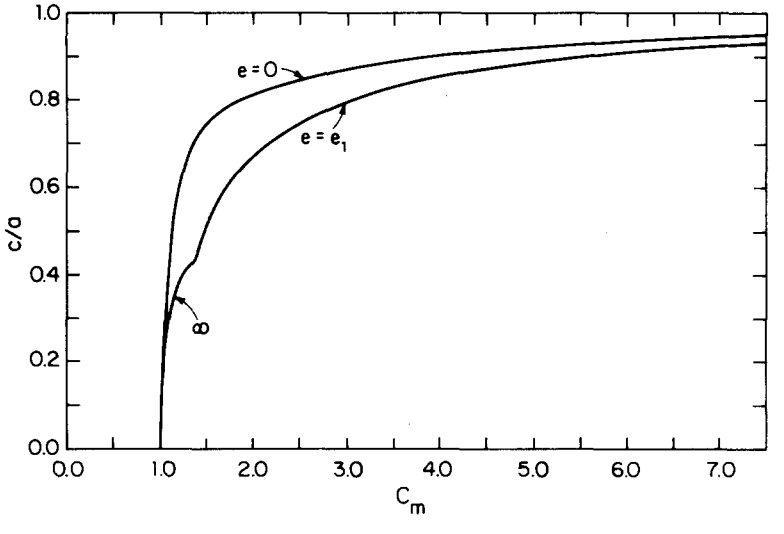

Figure 10. The moment coefficient C_m versus c/a.

6. A slightly deformed sphere

As spacing ratio c/a tends to zero, equations (9) and (10) reduce to

$$\frac{\omega a^3}{\beta c} = \frac{2\pi a^3}{(z^2+r_0^2)^{3/2}}\left\{\left[1+\frac{3(r_0^2-4z^2)c^2}{4(z^2+r_0^2)^2}+O\left(\frac{c}{a}\right)^4\right]\right.$$

$$\left.+\frac{c}{ea}\left[1+\frac{3(r_0^2-4z^2)c^2}{8(z^2+r_0^2)^2}+O\left(\frac{c}{a}\right)^4\right]\right\} \tag{22a}$$

and

$$\frac{\omega a^3}{\beta c} = 2\pi\left\{\left[1+\frac{3}{4}\frac{c^2}{a^2}+O\left(\frac{c}{a}\right)^4\right]+\frac{c}{ea}\left[1+\frac{3}{8}\frac{c^2}{a^2}+O\left(\frac{c}{a}\right)^4\right]\right\}, \tag{22b}$$

respectively. By neglecting terms of the order of $(c/a)^2$, (22) reduces to (11) which is the equation for a sphere of radius a as discussed in Section 4. However, if only terms of the order of $(c/a)^4$ are neglected, (22) is the governing equation for a slightly deformed sphere rotating about the z axis with an angular velocity ω. By (18) and (22b), the corresponding moment on this slightly deformed sphere is

$$\boldsymbol{M} = -8\pi\mu\omega a^3\left[1-\frac{3\left(1+\frac{1}{2}\frac{c}{ea}\right)}{4\left(1+\frac{c}{ea}\right)}\frac{c^2}{a^2}+O\left(\frac{c}{a}\right)^4\right]\boldsymbol{e}_z. \tag{23}$$

By neglecting terms of the order of $(c/a)^4$, a slightly deformed sphere given by (22) may be represented by a point rotlet with a vectorial strength

$$2\pi c(\beta+\alpha c)\boldsymbol{e}_z \tag{24a}$$

and a point rotlet-quadrupole with a vectorial strength

$$-\tfrac{1}{4}\pi c^3(2\beta+\alpha c)\boldsymbol{e}_z, \tag{24b}$$

both singularities being located at the origin. The velocity field due to a point rotlet located at the origin with a vectorial strength $\boldsymbol{e}_z$ is given by

$$\boldsymbol{u}_R(\boldsymbol{x};\,\boldsymbol{e}_z) = \frac{\boldsymbol{e}_z\times\boldsymbol{x}}{R^3} = \frac{r}{(z^2+r^2)^{3/2}}\boldsymbol{e}_\theta \tag{25}$$

and the velocity field for a rotlet-quadrupole is

$$\frac{\partial^2\boldsymbol{u}_R(\boldsymbol{x};\,\boldsymbol{e}_z)}{\partial z^2} = -3\frac{r(r^2-4z^2)}{(z^2+r^2)^{7/2}}\boldsymbol{e}_\theta. \tag{26}$$

The above results agree with the solutions of Jeffery [6], Brenner [1], and Chwang and Wu [3] for the limiting case of a spheroid as the eccentricity approaches zero.

7. A slender torus

A spinning slender torus discussed by Johnson and Wu [7] provides a special case for us to compare the results. We shall change the variables from z and r to ϵ and ψ by

$$z = -c\epsilon \sin \psi, \tag{27a}$$

$$r = c(1 + \epsilon \cos \psi). \tag{27b}$$

The body surface given by (7a) becomes

$$\epsilon = \epsilon(\psi), \tag{28a}$$

and the condition (7b) reduces to

$$\epsilon(0) = \frac{a - c}{c}. \tag{28b}$$

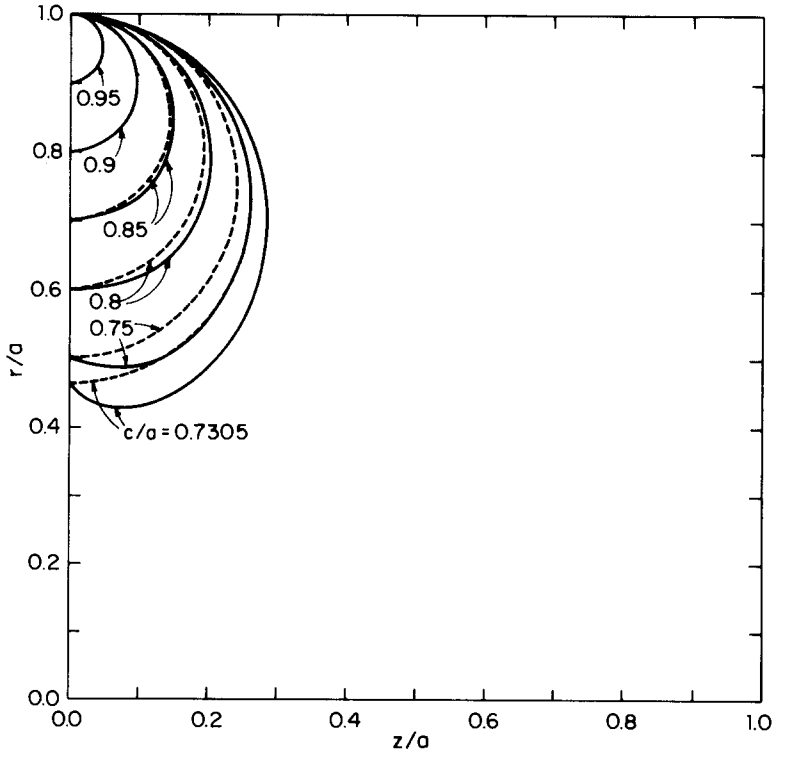

Figure 11. A comparison between exact class-B bodies (———) and circular tori (- - - - -).

For a slender torus, $\epsilon \ll 1$. Substituting (27) into (9a), comparing the constant terms and the cos ψ terms, and neglecting terms of $O(\epsilon^2 \ln \epsilon)$, we can determine the singularity strengths as

$$\alpha = \frac{\omega c}{4[\ln(8/\epsilon) - 2]}, \tag{29}$$

$$\beta = \alpha c \epsilon^2 [3 \ln(8/\epsilon) - 7]. \tag{30}$$

For a given body surface, ωc is a constant. Hence, ϵ must be a constant on the surface of a very slender torus. This constant is determined from (28b).

The above results agree exactly with the approximate solutions of Johnson and Wu [7] for a very slender torus of circular cross-section. Figure 11 shows a comparison between exact class-B bodies as computed from (9a) and circular tori. In Figure 11, the values of e for exact class-B bodies are so chosen that $t = 2c - a$. We note from Figure 11 that as c/a approaches one, the body becomes slender, and the body shape approaches that of a circular torus.

Acknowledgement

The first author, L.H. Huang, is grateful to the Graduate College of The University of Iowa for a research assistantship.

References

[1] Brenner, H. The Stokes resistance of a slightly deformed sphere, *Chem. Eng. Science* 19 (1964) 519–539.
[2] Chwang, A.T. Hydromechanics of low-Reynolds-number flow. Part 3. Motion of a spheroidal particle in quadratic flows, *J. Fluid Mech.* 72 (1975) 17–34.
[3] Chwang, A.T. and Wu, T.Y. Hydromechanics of low-Reynolds-number flow. Part 1. Rotation of axisymmetric prolate bodies, *J. Fluid Mech.* 63 (1974) 607–622.
[4] Chwang, A.T. and Wu, T.Y. Hydromechanics of low-Reynolds-number flow. Part 2. Singularity method for Stokes flows, *J. Fluid Mech.* 67 (1975) 787–815.
[5] Dorrepaal, J.M., Majumdar, S.R., O'Neill, M.E., and Ranger, K.B. A closed torus in Stokes flow, *Q.J. Mech. Appl. Math.* 19 (1976) 381–397.
[6] Jeffery, G.B. On the steady rotation of a solid of revolution in a viscous fluid. *Proc. Lond. Math. Soc.* 14 (1915) 327–338.
[7] Johnson, R.E. and Wu, T.Y. Hydromechanics of low-Reynolds-number flow. Part 5. Motion of a slender torus, *J. Fluid Mech.* 95 (1979) 263–277.
[8] Kanwal, R.P. Slow steady rotation of axially symmetric bodies in a viscous fluid, *J. Fluid Mech.* 10 (1961) 17–24.